JOURNAL OF GEOPHYSICAL RESEARCH, VOL. 112, C02001, doi:10.1029/2006JC003559, 2007

Alaska landfast sea ice: Links with bathymetry and atmospheric circulation

Andy Mahoney,[1,2] Hajo Eicken,[1] Allison Graves Gaylord,[3] and Lewis Shapiro[1]

Received 18 February 2006; revised 14 July 2006; accepted 8 September 2006; published 2 February 2007.

[1] Using Radarsat Synthetic Aperture Radar (SAR) imagery of northern Alaska and northwestern Canada, we calculated a mean climatology of the annual landfast ice cycle for the period 1996–2004. We also present the monthly minimum, mean, and maximum landfast ice extents throughout the study area. These data reveal where and when the landfast is most stable and which sections of the coast are susceptible to midseason breakout events. Stabilization of landfast ice is strongly related to the advance of the seaward landfast ice edge (SLIE) into waters around 18 m deep. Isobaths near this depth are a good approximation for midseason landfast ice extent. Comparison with work from the 1970s suggests a reduced presence of landfast ice in this region of the Arctic, due to later formation and earlier breakup. This will likely lead to an increase in coastal erosion and may also have profound effects upon subsistence activities, which are intimately linked to the timing of marine mammal migration patterns. Interannually, landfast ice formation correlates with the incursion of pack ice into coastal waters, suggesting that the later mean date of formation in recent years may be related to the increasingly northward location of the perennial sea ice edge. The timing of breakup correlates well with onset of thawing air temperatures. Analysis of regional data shows a multidecadal trend toward earlier thaw onset, which suggests that the observed change in breakup dates may be part of a longer-term trend.

Citation: Mahoney, A., H. Eicken, A. G. Gaylord, and L. Shapiro (2007), Alaska landfast sea ice: Links with bathymetry and atmospheric circulation, *J. Geophys. Res.*, *112*, C02001, doi:10.1029/2006JC003559.

1. Introduction

[2] In the Arctic, landfast sea ice is a key element of the coastal system, integral to a wide range of geological and biological processes as well as human activities. The presence of landfast ice can mitigate the effect of winter storms on the coast but also impede navigation in the spring. As well as being of great importance to native subsistence activities [*Nelson*, 1969; *George et al.*, 2004], the presence or absence of landfast in northern Alaska and its stability are of considerable economic importance for offshore development.

[3] Although multiyear landfast ice occurs in the Canadian Archipelago and has been observed in the Taymyr Peninsula [*Reimnitz et al.*, 1995], Arctic landfast ice is typically a seasonal phenomenon. The extent and appearance of landfast ice differ significantly across the Arctic. In much of Siberia, it extends hundreds of kilometers from the coast [*Zubov*, 1945; *Barnett*, 1991; *Eicken et al.*, 2005], compared to a width of roughly 5 to 50 km in the Alaska Arctic [*Barry*, 1979; *Stringer et al.*, 1980]. Water depths cited as coinciding with the limit of landfast ice extent vary by location: 25 m along the Siberian coast [*Zubov*, 1945], 10 m in the Kara Sea [*Divine et al.*, 2004], between 18 m and 30 m in the Beaufort Sea [*Canadian Hydrographic Service*, 1968; *Kovacs and Mellor*, 1974; *Reimnitz and Barnes*, 1974; *Stringer*, 1974; *Shapiro*, 1976; *Kovacs*, 1976; *Weeks et al.*, 1977; *Stringer et al.*, 1980], and 180 m off the eastern coast of Baffin Island [*Jacobs et al.*, 1975].

[4] This study focuses on northern Alaska and northwestern Canada (Figure 1a). In particular, we examine the relationship between water depth and landfast sea ice extent and the governing processes in different locations. Figure 1b shows the bathymetry within the study area as compiled by *Eicken et al.* [2006]. Point Barrow is the most prominent feature of the coast and marks the boundary between the Chukchi and Beaufort Seas. The western Beaufort Sea has the broadest expanse of water <20 m deep. In comparison, the seafloor slopes steeply away from the Chukchi coastline, particularly near Barrow Canyon. Mackenzie Trough is another prominent feature of the seafloor and holds the deepest waters near the coast in the study area.

[5] The temporal variability of landfast ice during its annual cycle is characterized by a gradual advance from the coast beginning in early winter followed by a rapid retreat in late spring. The formation of landfast ice is a complex process involving in situ freezing of open water in sheltered regions as well as the assimilation of pack ice

[1]Geophysical Institute, University of Alaska Fairbanks, Fairbanks, Alaska, USA.
[2]Now at National Snow and Ice Data Center, University of Colorado, Boulder, Colorado, USA.
[3]Nuna Technologies, Homer, Alaska, USA.

0148-0227/07/2006JC003559$09.00

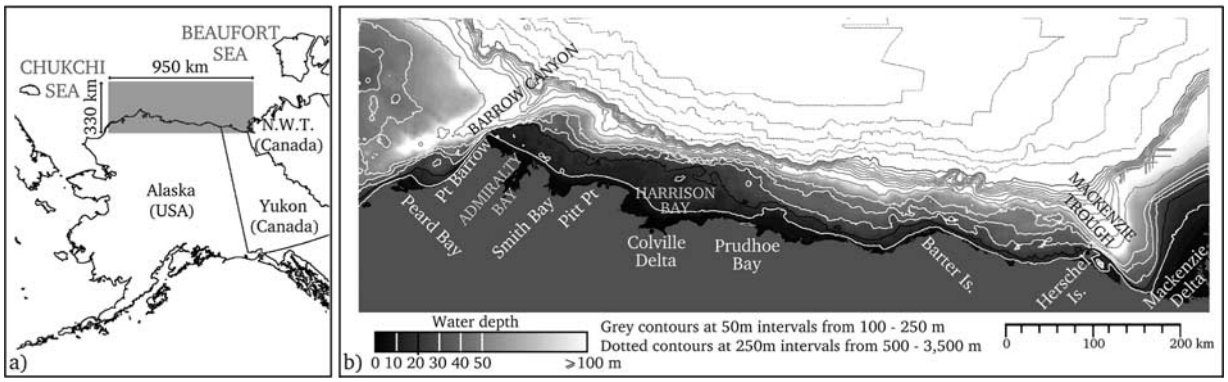

Figure 1. Study area and bathymetry. (a) The area of Alaska and Canada for which Radarsat SAR data were acquired.

from offshore. As a result, landfast ice grows seaward but may break up and reform a number of times before it achieves stability. The process of landfast ice breakup has received greater attention than that of formation, in part because of the difficulties of direct observations of freeze-up due to the darkness and inclement weather of Arctic fall and winter. With the onset of spring, increased air temperatures and downwelling radiative fluxes warm the snow and ice surface and initiate melt [*Persson et al.*, 2002] leading to a weaker ice cover. Eventually, the ice either melts in place or breaks up and drifts away following some combination of uplift of grounded ridges and offshore ocean and wind forcing.

[6] The small-scale processes controlling the response of landfast ice to external forcing are the subject of other ongoing research by the authors. Here, our aim is to identify the key linkages between landfast ice and coastal bathymetry and atmospheric forcing at the regional scale. First, we introduce methods to define landfast ice and determine the position of the seaward landfast ice edge (SLIE). We follow this by identifying four key events in the annual cycle: first ice on coasts; the onset of stable landfast ice; break-up; and the appearance of ice-free coasts. We then compare the timing of these events to a classification of regional atmospheric conditions including sea level pressure (SLP), freezing degree days (FDDs) and thawing degree days (TDDs). Having characterized the landfast ice in this fashion for recent years, we compare our results with those from earlier studies [*Barry et al.*, 1979; *Stringer et al.*, 1980] in order to address the causes underlying multi-decadal changes in Alaska landfast ice.

2. Methods

2.1. Delineation of the Seaward Landfast Ice Edge (SLIE)

[7] To quantify landfast sea ice variability, we applied a rigorous definition of landfast sea ice to remote sensing data. This definition derives from *Mahoney et al.* [2005] and is based on two criteria: (1) The sea ice is contiguous with the coast; (2) the sea ice exhibits no detectable motion for approximately 20 days.

[8] Criterion 2 implies that a single remote sensing scene is insufficient to identify landfast ice. The time interval of 20 days is a multiple of the average 10-day period between SAR mosaics (see below) and was chosen to represent a number of synoptic time periods, precluding sea ice that comes to rest temporarily against the edge of the landfast ice and lacks a mechanism to hold it fast. The time interval was also deemed to be operationally useful for planning activities on landfast ice. *Mahoney et al.* [2005] describe the application of this definition to identifying sea ice in Synthetic Aperture Radar (SAR) data and the implications of choosing different time periods. We exclude islands from our definition of the coastline, with the exceptions of Herschel and Barter Islands, which are larger than most others and separated from the mainland by only a very narrow stretch of water. This approach avoids complex topological problems when calculating distances from the coast, though it excludes ice that is not contiguous with the mainland but attached to barrier islands (which is of limited operational relevance and typically confined to late spring).

[9] Our definition was applied to Radarsat SAR data, acquired for the eight annual cycles between 1996 and 2004, covering the area shown in Figure 1a. Mosaics for this region were created from high-resolution ScanSAR data approximately every 10 days, as orbits allowed, between October and July. Each mosaic consisted of imagery spanning a 2 to 3-day period. In total, 238 mosaics provided between 28 and 35 mosaics per annual cycle. *Mahoney et al.* [2004] and *Eicken et al.* [2006] described the technique of applying the landfast ice definition to SAR data, involving examination of a set of three mosaics (spanning a period of ~20 days) and identifying regions with consistent backscatter patterns.

[10] The SLIE delineated in this fashion is a line representing the minimum offshore extent of contiguous stationary ice during the period represented by the three mosaics. We distinguish between a seaward and an inshore landfast ice edge. The latter develops during spring mostly in areas of bottomfast ice [*Reimnitz*, 2000], when river flooding and the development of an inshore lead can result in open water inside of the SLIE. Although the SLIE is defined for a given time period across the whole study area, a more specific date can be assigned at a specific location. The advancing SLIE is assigned the mean date of the first out of three mosaics. During landfast ice retreat, the defining date is the mean of the last mosaic. Since different parts of the landfast ice may be advancing and retreating at the same time, it is not meaningful to attribute a single date to the entire

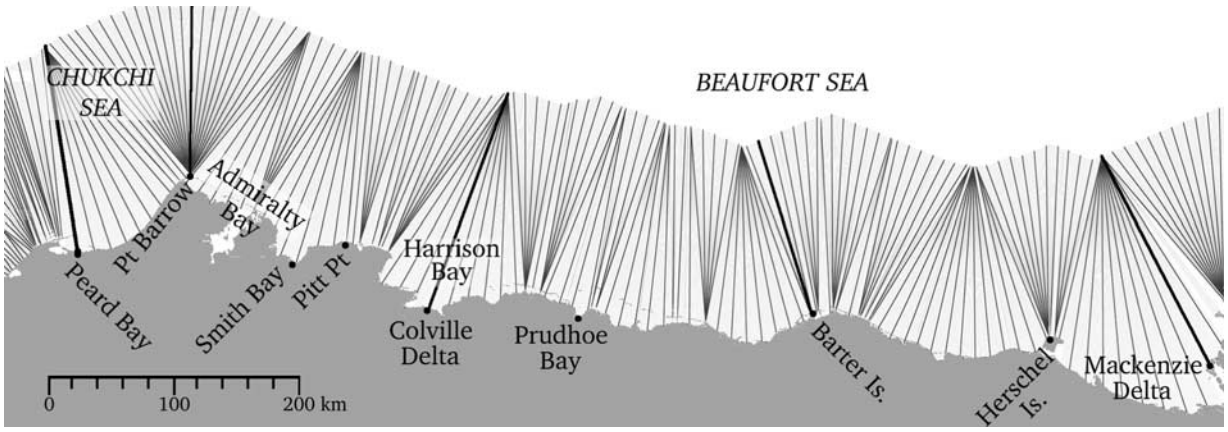

Figure 2. The transects along which landfast ice width is measured. Shown here is roughly every 10th line out of 1935 in total. Bold black lines indicate transects described in the text.

delineated SLIE. This delineation technique yields the shape of the SLIE and allows us to examine changes in landfast ice area over time. However, to quantify the variability in extent, we must define the position of the SLIE by measuring its width at different points along the coast.

2.2. Measuring Landfast Ice Width

[11] We measured landfast ice width along a set of transects defined in the following way. First, a line of offshore points was defined such that every point on the line was 150 km from the nearest point of land (excluding small islands). Every 1 km along this line, a point was connected by a transect to the nearest point on the coast so that some coast points were connected by more than one transect and others by none. Finally, those points on the coast lacking transects were connected to the nearest point on the offshore line to fill in concave regions of the coast. This process resulted in 1935 transects roughly perpendicular to the mainland coast along which the distance to the SLIE can be measured. These measurements are then binned into 200 groups for which average measurements were calculated (Figure 2).

[12] This approach works well for relatively simple coastlines. However, for more complex coastlines, with deep embayments, the line of offshore points must be closer to land, which limits the width of landfast ice that can be measured. The distance of 150 km chosen here strikes a balance between these two constraints. As a result, the waters of Admiralty Bay between Point Barrow and Pitt Point are not well represented and there are other small "shadows" behind headlands. Also, on rare occasions the SLIE was more than 150 km from the coast and measurements were truncated. This does not compromise the following analysis. The exclusion of small islands from our coastline means that ice attached to barrier islands, but separated from the mainland, is not included in the width measurement.

2.3. Identifying Key Events in Landfast Ice Development

[13] By calculating landfast ice width at 200 coastal locations (section 2.2), we charted the development of landfast ice during the eight annual cycles between 1996 and 2004. Figure 3 shows the time series of landfast ice width and water depth at the SLIE for a transect starting at the Colville Delta (see Figure 1b and Figure 2 for coastal locations) for the 2001–2002 cycle. Automated algorithms were then applied to these time series to determine the timing of four key events at each coastal location during each landfast ice cycle (Table 1).

[14] The selection of these four events is illustrated in Figure 3, but we note that not all annual time series fit this pattern and determination of all events was not possible for all locations in all years. Owing to restrictions of data availability, the date of the first mosaics acquired for each annual cycle varied. As a result, landfast was already present along an average of 67% of the coast in 1996, 1997, and 1998, when the first available mosaics were acquired latest in the year. In the remaining years this only occurred in 6% of time series. These occurrences and the entire first 3 years are excluded from the analysis of the dates of event 1.

[15] A detailed analysis (section 3.3) shows that the distribution of water depth along the SLIE is strongly modal, as illustrated by the dominance of water depths near 20 m in Figure 3. This supports the use of a specific water depth in the criterion for the landfast ice stabilization. For

Table 1. Key Events in Annual Landfast Ice Cycle

Event	Name	Description
1	first ice on coasts	The first occurrence of more than 500 m of ice at the coast represents the onset of ice formation, given the geolocation accuracy of the SAR imagery.
2	onset of stable landfast ice	Here, we define the stable period as the longest period during which the SLIE occupies water 15 m or deeper.
3	breakup	We define the occurrence of breakup by the fastest reduction in landfast ice width during the tail of the season once the landfast ice has ceased advancing. This does not necessarily coincide with the end of the stable period.
4	ice-free coasts	We deem the coast ice-free once the landfast ice width drops below 500 m.

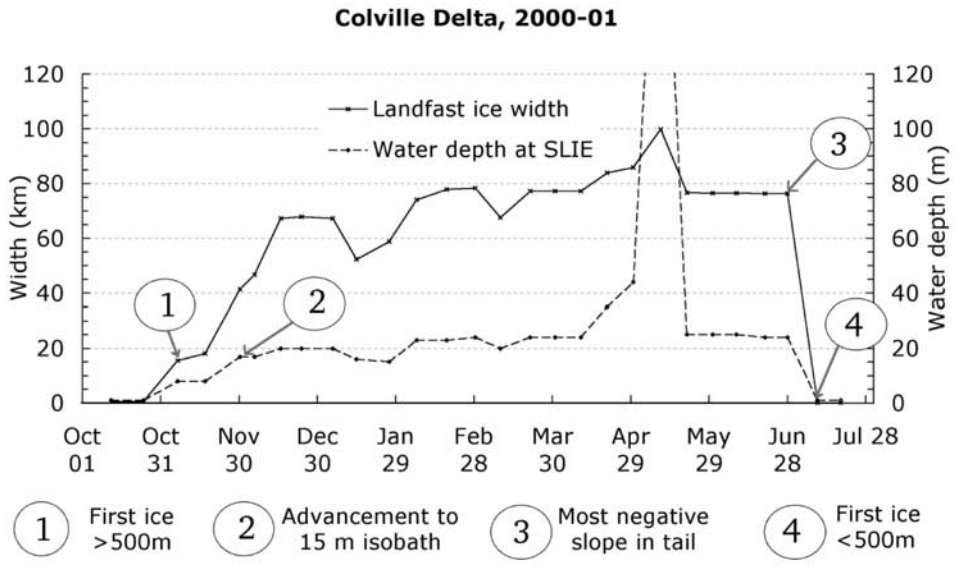

Figure 3. Development of landfast ice and water depth beneath the SLIE at the Colville Delta transect between October 2001 and July 2002. The numbered arrows show features of the time series that are used to determine the occurrence dates of four key events in the annual cycle.

the determination of event 2, a value of 15 m was chosen since this lies on the shallow side of the depth mode and once the SLIE advances into water depths > 15 m, it typically remains there until the end of the season. This is also the criterion for stability used by *Barry et al.* [1979], which aids the comparison of results. Using the 15 m depth criterion, determination of event 2 failed in 8% of instances. Determination of event 3 failed on 28% of occasions, mostly along coasts with a narrow belt of landfast ice. Event 4 remained unobserved for <1% of all measurements. In all these cases, the results were excluded from subsequent analysis.

[16] The algorithms described above will always give the date of the first mosaic in which the event is observed, which may be up to 10 days after the actual occurrence. To compensate, the dates used in the subsequent analysis are all shifted back by 5 days, resulting in an error of ±5 days for each event.

2.4. Objective Synoptic Classification

[17] Using an objective classification scheme, we identified Characteristic Patterns (CPs) of sea level pressure (SLP) using mean daily fields acquired from the National Centers for Environmental Prediction (NCEP) data set. All data available up to the end of the study period were acquired (1948–2004), over an area extending from 55° to 80°N and 180°–120°W. In the classification scheme, each daily field is normalized by subtracting its mean and dividing by its standard deviation. A difference value, determined by the sum of the square of the differences between corresponding grid cells is used to quantify the similarity between two fields. Details of this calculation are given by a number of authors [*Kirchhofer*, 1974; *Barry*, 1976; *Barry*, 1979; *Barry and Carleton*, 2001; *Serreze and Etringer*, 2003]. Two daily pressure fields with difference values below certain thresholds are deemed similar. Individual fields with more than five other fields similar to them are identified as characteristic patterns (CPs). Other fields are then assigned to the CP with which they share the lowest difference value.

[18] The CPs are then placed in order so that CP 1 has the most fields assigned to it. We chose the same threshold difference values as *Barry* [1979] and obtained 60 CPs characterizing the 20,820 daily fields between 1948 and 2004. Each CP represents a group of SLP fields with a similar distribution of high and low pressure systems. The normalization step reduces the influence of the magnitude of a pressure gradient. It is therefore difficult to infer specific weather conditions resulting from each CP, but it is possible to gauge the general pattern of airflow and the time of year with which a given CP is usually associated.

2.5. Freezing and Thawing Degree Days

[19] Accumulated freezing and thawing degree days were calculated from NCEP air temperatures at each of the 200 coast points (Figure 2) through bilinear interpolation of the surrounding NCEP grid cells. Freezing degree days (FDDs) were calculated by summing the daily mean air temperatures of days with mean temperature below 0°C since the onset of freezing. We defined the date of the onset of freezing as being the first day with an average temperature below zero that is also the first day of a 15-day period that has an average temperature below 0°C. Thawing degree days (TDDs) and the onset of thawing were defined similarly for days with temperatures above 0°C.

3. Results

3.1. Location of the SLIE

[20] Delineation of complete SLIEs within the study area over 8 years allowed us to examine the spatial and temporal variability of the landfast ice. Figure 4 shows the landfast

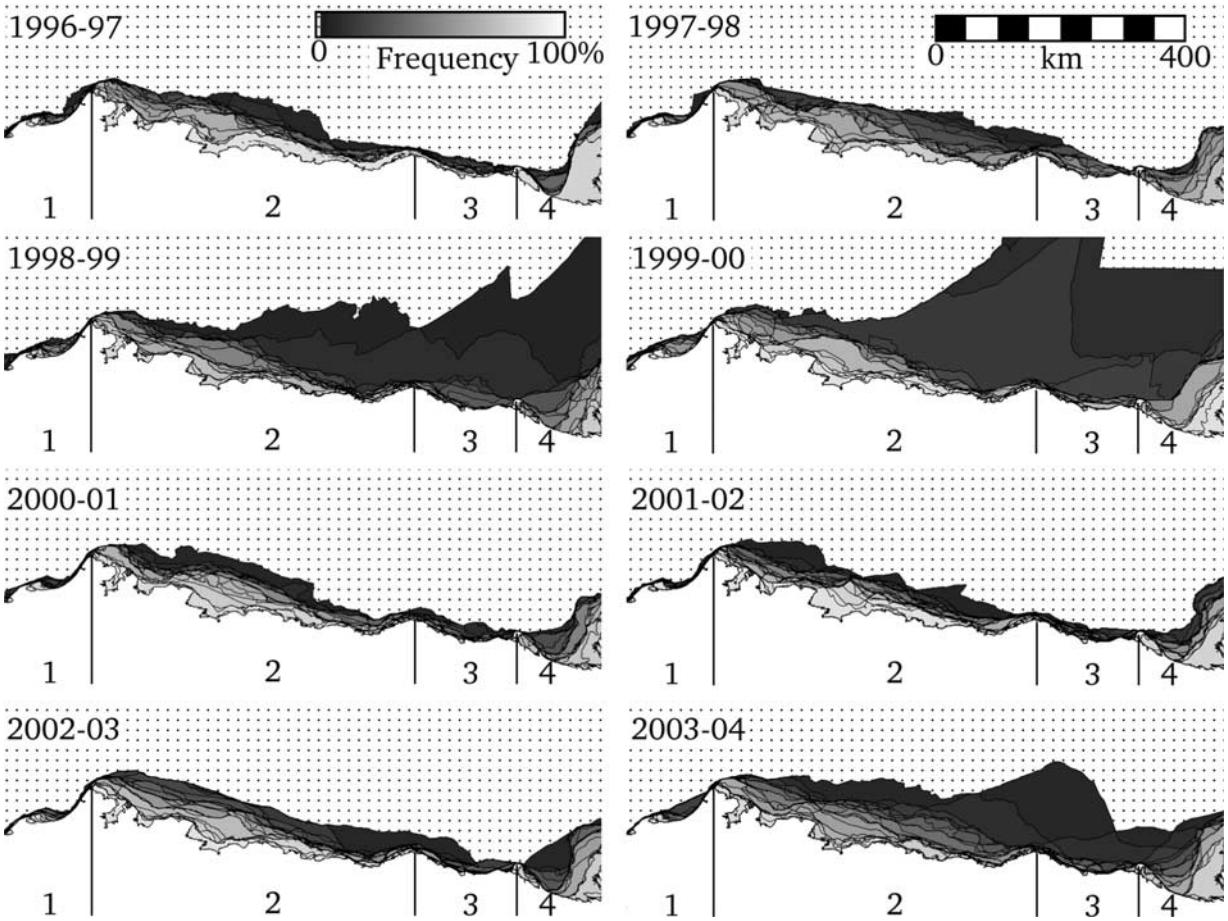

Figure 4. The locations of all SLIEs for each year. The landfast area shoreward of each SLIE is stacked such that the grey shade of the area represents the fraction of the annual cycle (October–July) for which that area was occupied by landfast sea ice. The numbers 1–4 indicate the locations of the zones described in section 3.1. The darkest shades indicate the maximum extent of landfast sea ice in that year. The dotted area indicates where landfast ice was never observed. The black lines indicate the locations of the individual SLIEs.

ice areas shoreward of each SLIE compiled by year such that the grey value indicates the relative frequency with which landfast ice was observed at any point in the study area for each annual cycle. The individual SLIEs for each year appear in black and are similar to frequency contours. Areas with a high spatial density of SLIE locations correspond to low variability in landfast ice extent, which in turn corresponds to greater landfast ice stability. The darkest areas indicate the maximum extent of landfast ice in each year. Interannual differences are dominated by vast extents of motionless ice, which we refer to as stable extensions following *Stringer et al.* [1980] and discuss further in section 3.5.

[21] Across the study area, differences in landfast ice extent and the density of SLIEs, allow four zones to be distinguished (Figure 4). To the west of Point Barrow, in the Chukchi Sea (Zone 1), the landfast sea ice occupies a much narrower strip and the SLIEs appear more densely spaced than to the east in the western portion of the Beaufort Sea (Zone 2). Zone 3 extends between Barter and Herschel Islands, where the landfast ice extent and variability resemble that of the Zone 1 except during those occasions when large stable extensions of landfast ice occur. Zone 4 lies east of Herschel Island in an area in which the Mackenzie River and the coastline of the Mackenzie Delta influence the ice.

[22] In addition to these four zones, there are smaller-scale variations in the spatial density of SLIEs, particularly in Zone 2 in the western Beaufort Sea where there appear to be discrete nodes at which the SLIEs converge. These nodes have been described by *Mahoney et al.* [2005] and indicate localized stabilization of the landfast ice. The strong correlation between the 20 m isobath (Figure 1b) and areas of high SLIE density suggests that these nodes correspond to locations where the SLIE is pinned by grounded ridges. The role of bathymetry in confining the SLIE will be examined in more detail in section 3.3.

3.2. Monthly Landfast Ice Extents

[23] Figure 5 illustrates the mean annual cycle of landfast ice and its variability across the study area. Details of calculating the monthly minimum, mean, and maximum SLIE positions are given by *Eicken et al.* [2006]. Landfast ice grows gradually from October through to February with the greatest monthly mean extent occurring in March and

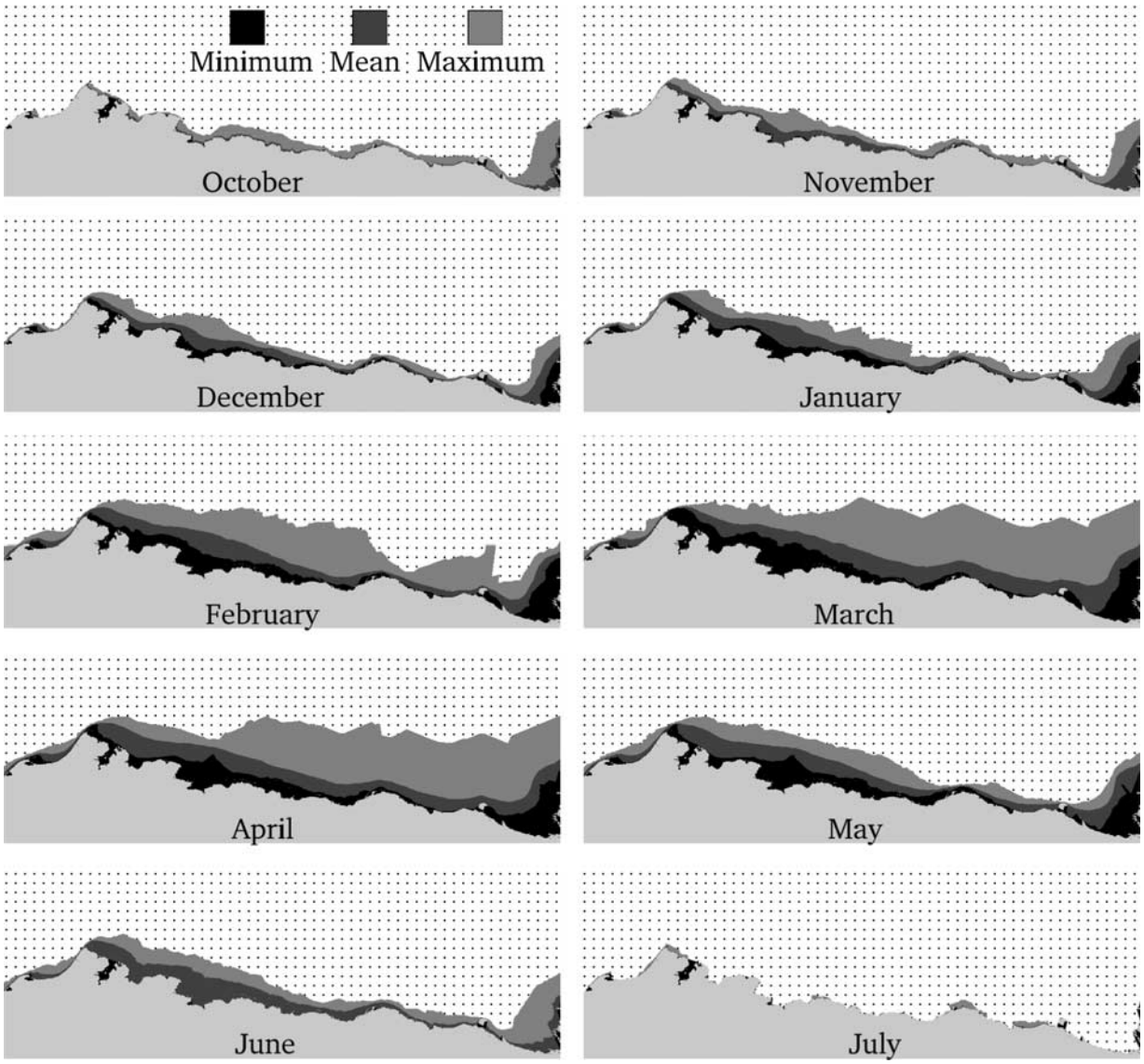

Figure 5. Minimum, mean and maximum monthly mean landfast sea ice extents showing the change in landfast ice distribution through the annual cycle. The dotted area indicates where landfast ice was never observed.

April for most of the study area except for the central portion of Zone 2 (see Figure 4 for zone locations), where it is greatest in May. March and April show the greatest difference between the monthly mean and maximum extents, which reflects the occurrence of stable extensions (section 3.5) during these months. The real extents of these stable extensions are truncated by the width measurement technique (section 2.2) and so do not appear in Figure 5.

[24] The expansion of landfast ice is not a continuous process and can involve many stages of formation, breakup, and reformation. Except for October, when the landfast ice may not have had time to form and break up, the monthly minimum SLIE corresponds to most severe breakout that was observed in any month. Figure 5 shows that through March, the minimum SLIE position advances behind the mean indicating that breakouts become less severe. Breakouts become severe along some parts of the coast beginning sometime in April. This is most obvious in the western Beaufort Sea between the Colville Delta and Point Barrow, suggesting this region is more susceptible to breakouts. By contrast, the area north of Harrison Bay remains stable until June and represents the most seaward monthly minimum position of the SLIE. The tip of this area corresponds to one of the nodes that can be seen in Figure 4 and lies above a local shoal.

3.3. Water Depth at the SLIE

[25] Figure 1b shows the gridded bathymetry dataset used in this study, with the 20 m isobath shown in black. The 20 m isobath often coincides with consistent SLIE locations in this region [*Reimnitz and Barnes*, 1974; *Shapiro*, 1976; *Kovacs*, 1976; *Stringer et al.*, 1980]. In certain months, its position and shape closely resemble those of many of the 222 SLIEs delineated in this study. Using these bathymetry

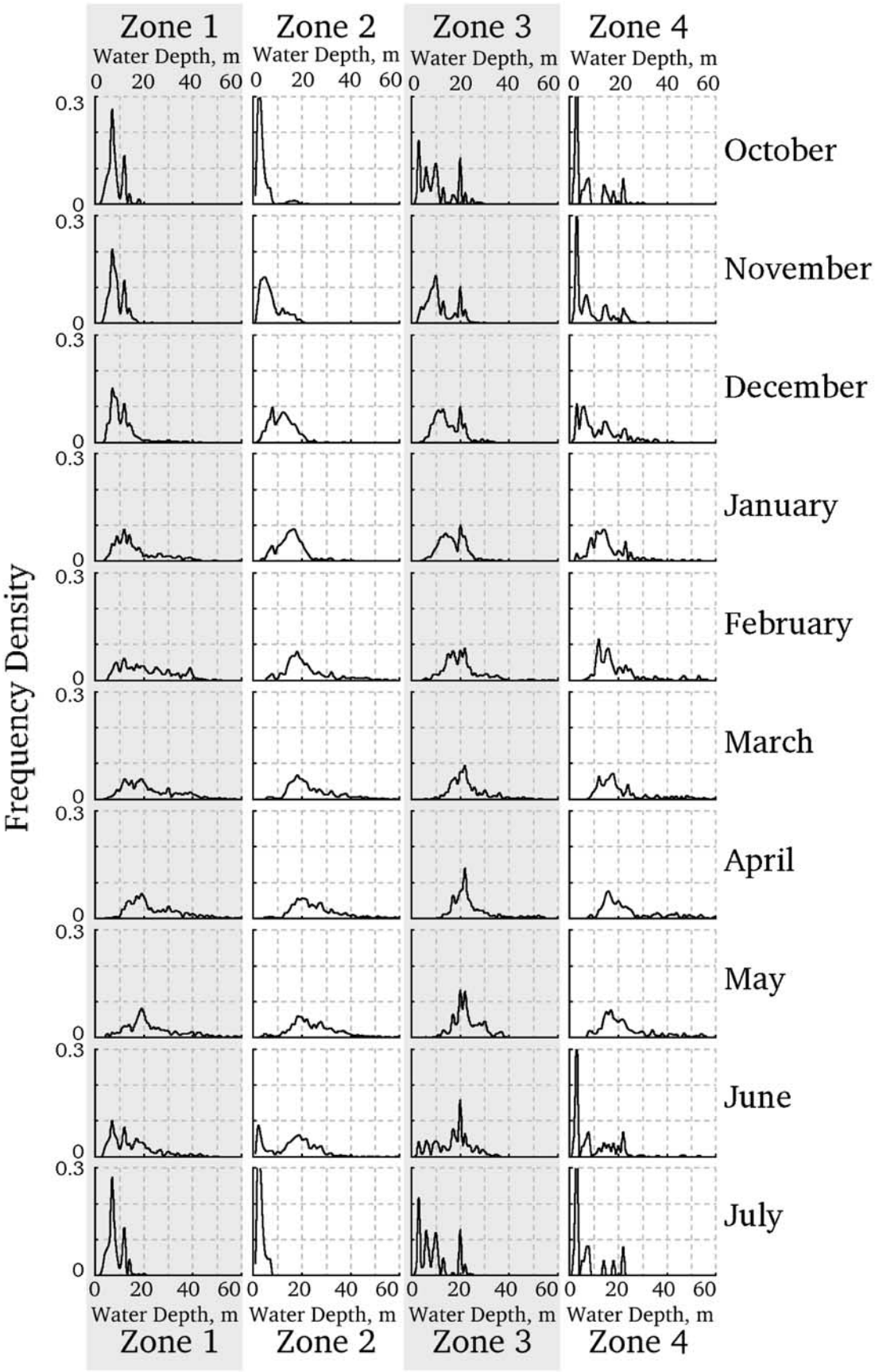

Figure 6. Monthly histograms of water depth at the SLIE for each of the four zones identified in section 3.1.

Table 2. Modal Water Depth at the SLIE at the End of Winter for Each Zone and the Month in Which This Distribution Is Achieved

	Zone 1	Zone 2	Zone 3	Zone 4
Final modal water depth at SLIE	19 m	18 m	22 m	16 m
Month achieved	Apr	Jan	Feb	Mar

data and the transects shown in Figure 2, we measured the variability of water depth at the SLIE.

[26] Figure 6 shows the distribution of water depths occupied by the SLIE in each of the 4 zones and how this varies through each month of the annual cycle. In all zones, the SLIE advances into deeper water and the histograms evolve toward a unimodal distribution by the end of winter. However, each zone differs according to depth of this mode and the time of year in which it is achieved. Table 2 summarizes these differences. We assume that water depths in which the SLIE is most frequently observed correspond to depths in which the SLIE is most stable. Occupation of the modal water depth is a useful indicator of stability of the landfast ice, since the histograms do not change significantly once the mode has reached such a depth. However, as stated in section 2.3, a depth of 15 m was chosen to indicate the onset of stabilization in keeping with the work of *Barry et al.* [1979] and to reduce the sensitivity of the stability criterion.

[27] As with the expansion of landfast ice area, the advance of the SLIE into deeper water is more gradual and episodic than its retreat at the end of the annual cycle. In fall, the distributions in all zones are multimodal with an absolute maximum in shallow water. In later months, the SLIE advances from one stable water depth to the next until it reaches its final modal depth. Furthermore, the October and July distributions are strikingly similar for all zones, suggesting that although the retreat is more rapid, the SLIE reoccupies the same water depths as during its advance.

[28] Figure 7 shows the monthly mode and range of water depths occupied by the SLIE as measured along each transect, detailing spatial variability across the study area. Throughout the first few months of the annual cycle, more points advance to water depths indicated by the envelope of the previous month. This suggests the SLIE as a whole advances from one modal water to the next through a process whereby separate sections advance first, allowing the neighboring sections to catch up later. Figure 7 also helps explain the significance of the modal water depths indicated in Figure 6 and Table 2, particularly in Zone 2. Before the SLIE in each zone advances to these depths, very little of the SLIE extends into deeper waters. However, there is a clear transition once a significant fraction of the SLIE occupies the modal water depth for that region. It is only afterward that landfast is commonly found in water deeper than the modal depth and is rarely found in shallower water. This is a further indication that stability is strongly linked to bathymetry.

3.4. Key Events Within the Annual Cycle

[29] By examining annual variation in landfast ice width along the transects shown in Figure 2, we determined the mean occurrence dates over the study period of the four key events described above (Figure 8). Determination of the occurrence date of each event was not possible for every year for every point along the coast (section 2.3). Typically, the mean dates shown in Figure 8 are calculated from at least six annual cycles, with the exception of the onset of first ice (event 1) for which only the last five annual cycles were used.

[30] Figure 8 indicates that there is both regional and local variability in the timing of key events. Broadly, the date curve for the first occurrence of ice is "u"-shaped, with landfast ice typically forming first in Zone 2 and later to the east and west. We see the inverse pattern ("n"-shaped curves) in the timing of breakup and ice-free conditions. The date curve for stabilization of the landfast ice is not shaped like the others and has far greater standard deviations. Some regions of the coast stabilize significantly earlier than others, with most of zone 2 stabilizing earliest, beginning with Prudhoe Bay. There is also some evidence of a sawtooth pattern with stabilization progressing westward from those locations that stabilize earliest. This is in agreement with earlier observations of the development of shear zones from Landsat-1 imagery [*Reimnitz et al.*, 1978].

[31] In addition to broad regional trends, we also see higher-frequency spatial variability related to coastal morphology and bathymetry. For example, in the shelter of Peard Bay, landfast ice forms significantly earlier than on the coasts nearby, though the effect of the inflow of the Kugrua River here is not known. The earliest offshore points to stabilize correspond to the locations of shoals (Figure 1b). Such signals can be distinguished from scatter in the data by examining the standard deviations. Furthermore, the four coastal zones exhibit distinct differences in the magnitude and character of the high-frequency spatial variability in the date-curves. This is most obvious in the case of Zone 2, where the standard deviations and range of dates are smallest and the mean date curves are generally smoothest. Thus the landfast ice cycle of the western Beaufort Sea is the most regular and uniform. Zones 1, 3, and 4 by comparison exhibit greater interannual variability and a stronger influence of local coastal morphology.

[32] The dates of the key events exhibit much greater spatial variability than the onset of freezing and thawing, indicating that there is no single relationship between the accumulation of FDDs and TDDs and the timing of the annual cycle. Figure 9 shows the mean degree days accrued at the time of each key event and the standard deviations for each zone. Zone 1 requires more FDDs to acquire its first ice than the other zones and less TDDs to incur breakup and ice-free conditions. Figure 9 also shows the mean values calculated at points located on headlands or open coasts and in embayments or lagoons. These suggest that at least part of the variability can be explained by coastal morphology. In Zones 1, 3, and 4, landfast ice in embayments generally forms before and breaks up after ice on headlands. Coastline effects are less pronounced (and in fact reversed for breakup) in Zone 2, suggesting that offshore bathymetry is more important in this zone.

[33] Examination of the occurrence dates throughout the study period reveals no strong temporal trends. Longer-term changes are examined in Table 3, comparing key seasonal events from this study to those of *Barry et al.* [1979] for the period 1973–1977. Of the eight events Barry et al. identi-

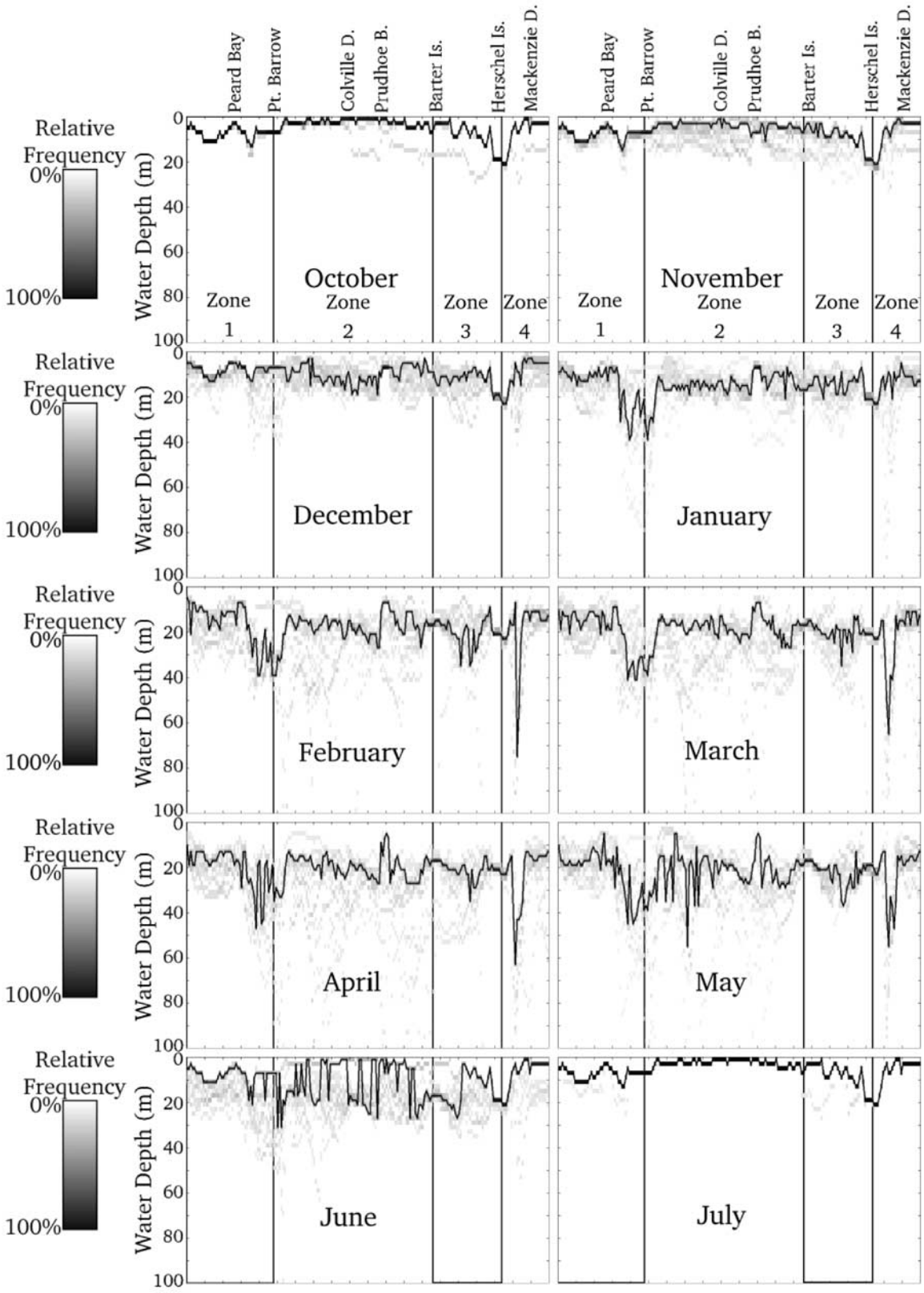

Figure 7. Detailed spatial variability in modal water depth at the SLIE for each month. The black curve shows the monthly modal water depth at each coastal location. The histogram of depths occupied by the SLIE at each location is illustrated by the grayscale. Note that the very deepest waters beneath stable extensions (section 3.5) extend beyond the axes and are not shown. The vertical black lines indicate the extents of the four previously identified zones (Figure 4).

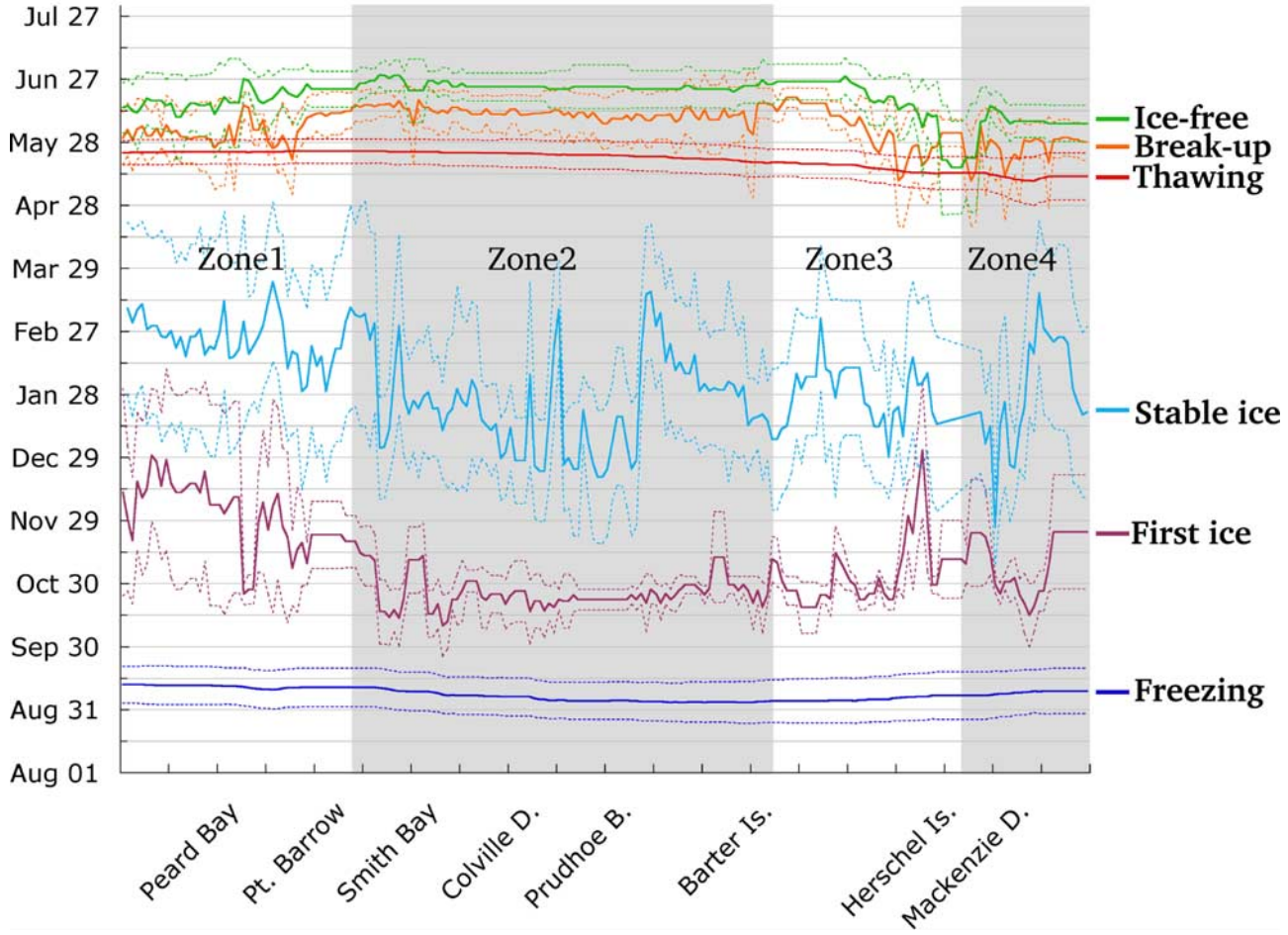

Figure 8. Spatial variability in the dates of occurrence of four key events in the annual cycle and the onsets of freezing and thawing derived from surface observations. The bold lines indicate the mean for the study period and the dashed lines indicate ±1 standard deviation from the mean. The x-axis represents the 200 coastal locations from west to east (see Figure 2) and the shading indicates the extents of the four zones identified in section 3.1.

fied, we have chosen the four that most closely match ours. The regions denoted as central Chukchi and central Beaufort by Barry et al. correspond to our Zones 1 and 2, respectively. Each date calculated in this study has an error of approximately ±5 days, while *Barry et al.* [1979] estimate errors of ±10–15 days relative to the mean.

[34] Table 3 indicates that formation of landfast ice occurs approximately 1 month later along the Chukchi coast than in 1973–1977, with little change along the central Beaufort Coast. Both of these differences are within the range of uncertainty, however. The timing of stabilization has not changed greatly since the 1970s, though the dates given by *Barry et al.* [1979] for this event are not specific. In recent years, breakup occurred earlier with a difference of 6 and 21 days along the Chukchi and Beaufort Sea coasts, respectively. Although the description given by Barry et al. for "first openings and movement" qualitatively matches the criterion that defines breakup in this study, the dates given here are an average of those calculated for all coastal points within each zone. Using the date on which breakup was first observed in each zone, rather than the mean date, gives a breakup date approximately 3 weeks earlier than the dates in Table 3, which would represent a significant shortening of the stable landfast ice period since the 1970s.

[35] Ice-free coastlines now occur over a month earlier along the Beaufort Sea coast and approximately 2 weeks earlier along that of the Chukchi Sea. In the latter case, this is barely significant. However, the magnitude of the change in the Beaufort Sea is clearly significant.

3.5. Episodic Events

[36] We use the term episodic events to refer to the brief events that occur at irregular intervals and result in a deviation of the SLIE position from the mean annual cycle. The Radarsat imagery used in this study allows us to identify breakouts and stable extensions, where the SLIE lies briefly landward or seaward of its normal position. Significant stable extensions occurred in the Beaufort Sea on 5 occasions in 4 different years (Figure 4, Table 4). Although others observed similar features [*Barry*, 1979; *Barry et al.*, 1979], they are not typically considered part of the landfast ice. We include them here in keeping with our definition (section 2.1).

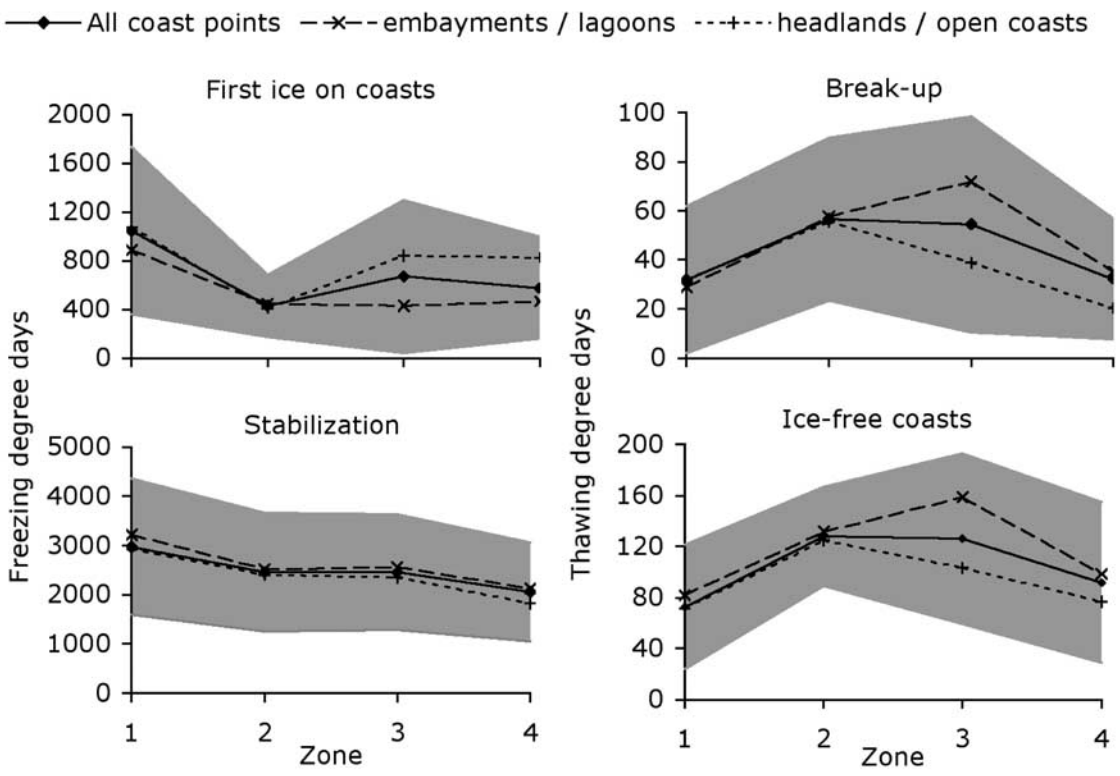

Figure 9. The mean number of degree days accrued at the time of each event in each zone. The results are also broken down according to whether a point on the coast lies on a headland or in an embayment. The shaded area indicates one standard deviation either side of the mean for all points.

[37] Stable extensions occur most frequently in March and April in the eastern half of the study area, at the time of greatest sea ice concentration. On these occasions, the SLIE lies in water up to 3500 m deep, but *Mahoney et al.* [2005] speculated that the sea ice may be anchored somewhere outside of the study area in the vicinity of Banks Island. *Stringer et al.* [1980] noted that landfast ice could extend up to 100 km offshore in the absence of disturbance, though *Thorndike and Colony* [1982] observed such events despite strong winds. It is beyond the scope of this study to consider all the stresses on the ice sheet during these stable extensions, but section 4.2 discusses their correlation with other aspects of landfast ice behavior.

[38] On the basis of the Radarsat imagery processed for this study, *Blazey et al.* [2005] identified 267 breakout events and categorized them according to severity based upon the fraction of the landfast ice width involved and the depth to which the SLIE retreated. Most severe breakouts occur in July and coincide with the annual breakup of the landfast ice, but some were observed at other times of the year, though without any clear pattern of timing. The spatial pattern of breakouts suggests that the eastern region of Zone 2 is least susceptible to such events, while several breakout events affected the ice immediately east of Point Barrow. These breakouts are responsible for the more shoreward location of the monthly minimum SLIE positions

Table 3. Mean and Mean Interannual Standard Deviation, σ', of the Occurrence Dates for the Four Key Events of the Annual Landfast Ice Cycle for Each Zone

		1996–2004 (This Study)					1973–1977 [*Barry et al.*, 1979][a]		
		Zone 1	Zone 2	Zone 3	Zone 4	All Zones	Central Chukchi	Central Beaufort	
First Ice[b]	Mean	Dec 01	Oct 25	Nov 04	Nov 9	Nov 7	Early November	Mid October	First continuous fast ice
	σ'	31.8	9.6	11.4	17.5	16.4			
Stable Ice	Mean	Feb 23	Jan 22	Jan 28	Jan 27	Feb 01	Feb	Jan/Feb	Stable ice inside of 15 m isobath
	σ'	41.9	30.1	32.6	34.9	34.1			
Breakup	Mean	Jun 04	Jun 11	Jun 04	May 26	Jun 06	Jun 10	Jun 30	First openings and movement
	σ'	13.9	14.2	13.7	12.6	14.6			
Ice Free	Mean	Jun 18	Jun 24	Jun 24	Jun 06	Jun 18	Jul 05	Aug 01	Nearshore largely free of fast ice
	σ'	12.7	8.4	12.6	10.2	10.4			

[a]The occurrence dates for the events most closely matching ours are given. The Central Chukchi and Central Beaufort regions correspond to Zones 1 and 2, respectively, in our study.
[b]1996–1998 omitted from analysis (see section 2.3).

Table 4. Dates of occurrence of stable extensions observed in this study[a]

First Date of First Mosaic	Last Date of Last Mosaic	Duration, days	Location
1999/04/04	1999/04/26	22	Prudhoe Bay – Mackenzie Delta
2000/02/23	2000/04/08	44	Pitt Point – Mackenzie Delta
2001/04/29	2001/05/22	24	Smith Bay – Prudhoe Bay
2004/02/15	2004/03/08	22	Colville Delta – Prudhoe Bay
2004/02/25	2004/03/18	22	Barter Island – Mackenzie Delta

[a]Note that the mosaic dates (section 2.1) give the earliest and latest dates we observed the extension, which may therefore underestimate the duration by up to approximately 20 days.

in this area (Figure 5). The mechanisms of winter breakouts likely differ from those occurring at the end of the season when the landfast ice is weaker.

3.6. Characteristic Synoptic Climatology

[39] As stated in section 2.4, we categorized the synoptic variability over Alaska for the period 1948–2004 into 60 characteristic patterns (CPs). Using the same methodology and parameters, *Barry* [1976, 1979] and *Moritz* [1979] derived 21 CPs for the period 1969–1974. Overall, we observe the same range of variability in sea level atmospheric pressure patterns and the three most prevalent CPs from our study resemble the most prevalent CP of the earlier analysis. No patterns identified by Barry and Moritz are obviously absent from our results, though the exact orders of prevalence do not agree. *Moritz* [1979] describes the

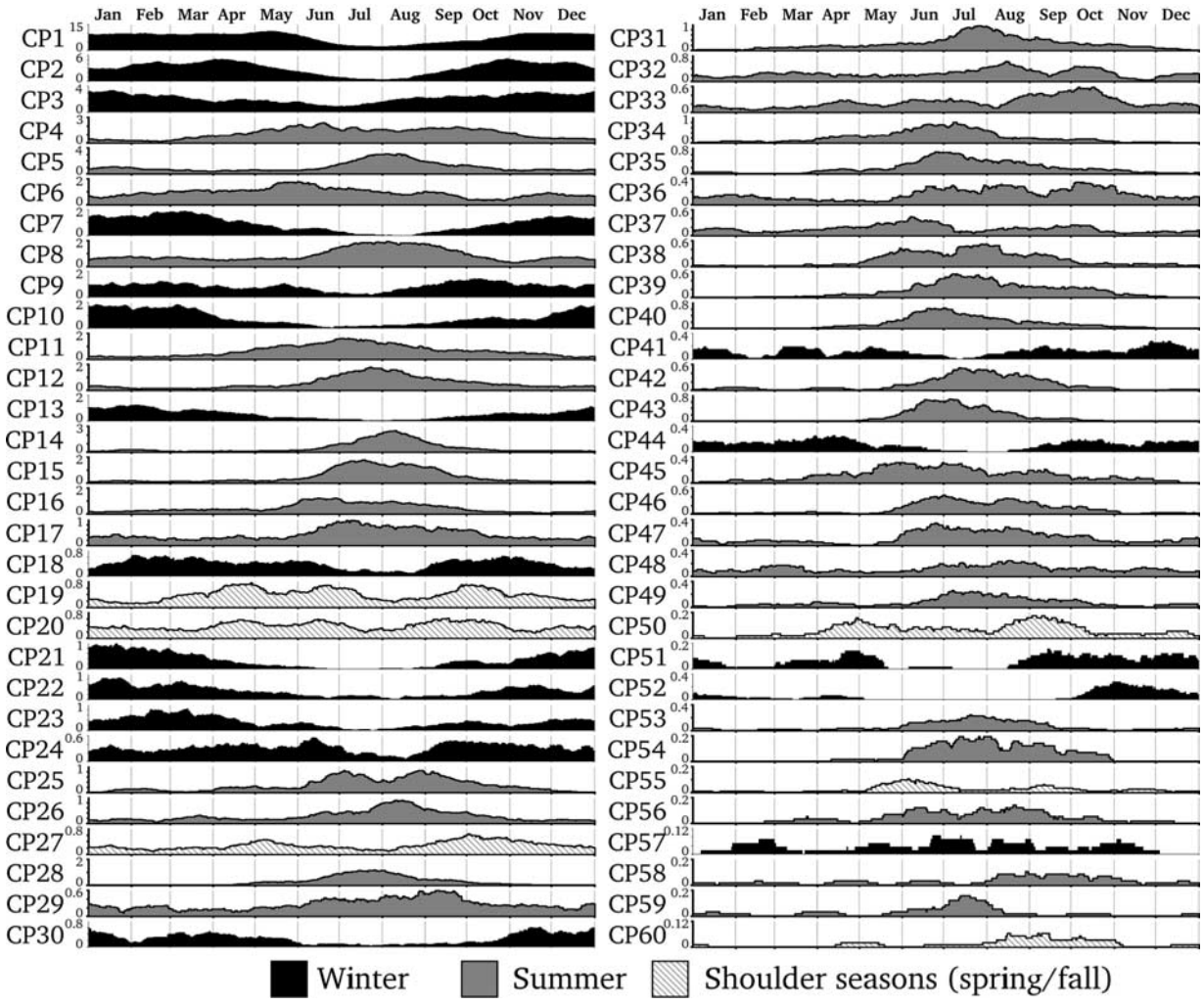

Figure 10. Running 31-day means of the occurrences of each characteristic pattern (CP) after binning according to day of year. This quantity is taken to represent the monthly occurrence frequency for each CP. Each plot is shaded according to whether it occurs mostly in the winter (black), summer (gray), or the shoulder seasons (hatched). Note different scales on each y-axis.

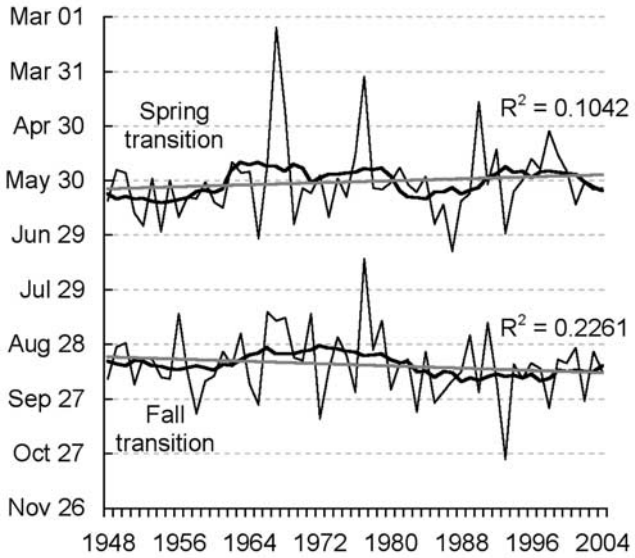

Figure 11. The dates of the spring and fall transitions determined from the ratio of winter to summer CPs. The bold curve shows a 10 year running mean of these data and the grey line is a linear regression of the 10-year running mean of this data (bold curve) with the corresponding R2 values.

general characteristics of each CP for period 1969–1974, together with the general pattern of air flow. While it is possible to do the same for our results, it is difficult to interpret specific weather conditions and how these would affect the landfast ice. No statistical relationship was found between the occurrence of SLP patterns corresponding to a given CP and an event in the landfast ice. Here, we analyze the CP results for evidence of change in the synoptic regime over Alaska.

[40] Figure 10 shows the 31-day running mean of the occurrences of each CP, binned by day of year. It is striking that every CP appears modal or bimodal in its annual distribution. This allows the majority to be categorized as either a winter or summer pattern, with just six CPs that show peaks in the transitions between summer and winter (shoulder seasons). *Moritz*'s [1979] results show a similar seasonality. In this part of the world, winter SLP patterns are characterized by a high pressure in the north and low pressure systems in the south [*Barry*, 1979]. In summer, central, western, and northern regions typically exhibit low pressure patterns while the Pacific High often extends as a ridge over the Gulf of Alaska. Examination of each CP shows that most fit the description for the season in which they most frequently occur. With a few exceptions, this strong seasonality of the data supports our characterization of the synoptic climatology.

[41] We did not find any significant temporal trends or regime shifts in the occurrence frequencies of individual CPs. However, by further grouping each CP into winter, summer and shoulder season categories, we examined changes in the seasonal weather patterns experienced by landfast ice. This seasonal categorization was made according to the season in which each CP most frequently occurred (Figure 10). Using this, we calculated the ratio of winter to summer CPs over a running 90-day period. This ratio exhibited an obvious annual period, which allowed us to identify the timing of the spring and fall transitions each year. These were defined as the day of year when the ratio rose above and fell below 0.5, respectively. Variability in the timing of the spring and fall transitions derived from the CP data is shown in Figure 11. Linear regressions indicate weak trends toward earlier springs and later falls, however there is strong interannual variability. *Mahoney* [2006] also calculated the contribution of summer, winter, and shoulder season CPs to each month. These results indicate that in terms of SLP patterns, Septembers and Octobers of recent years resemble Augusts and Septembers from earlier in the period.

3.7. Freezing and Thawing Trends

[42] Extending the analysis of seasonal landfast ice events in the context of freezing and thawing (section 3.4), Figure 12 shows the variation over time of the dates of onset of freezing and thawing and total degree days accumulated in each year. The solid black curves show values derived from NCEP data interpolated for Point Barrow (section 2.5), while the dashed black curves show values calculated using the same method with data from Barrow Wiley Post Airport weather station for the period 1984–2004 (the period available online from the National Climatic Data Center). The results from the two datasets differ in the magnitudes of largest peak values but otherwise are well correlated and converge in recent years.

[43] Despite substantial interannual variability (discussed in section 4.2), both datasets show strong trends (significant at the 98% level) toward a later onset of freezing and warmer winters. There are also weaker trends (but still significant at the 98% level) toward earlier onsets of thawing and warmer summers. The grey curves show the running 8-year means of the NCEP-derived values, for which the black lines illustrate linear regressions. While these trends may have far-reaching implications, we will limit our discussion to the impacts on landfast ice and

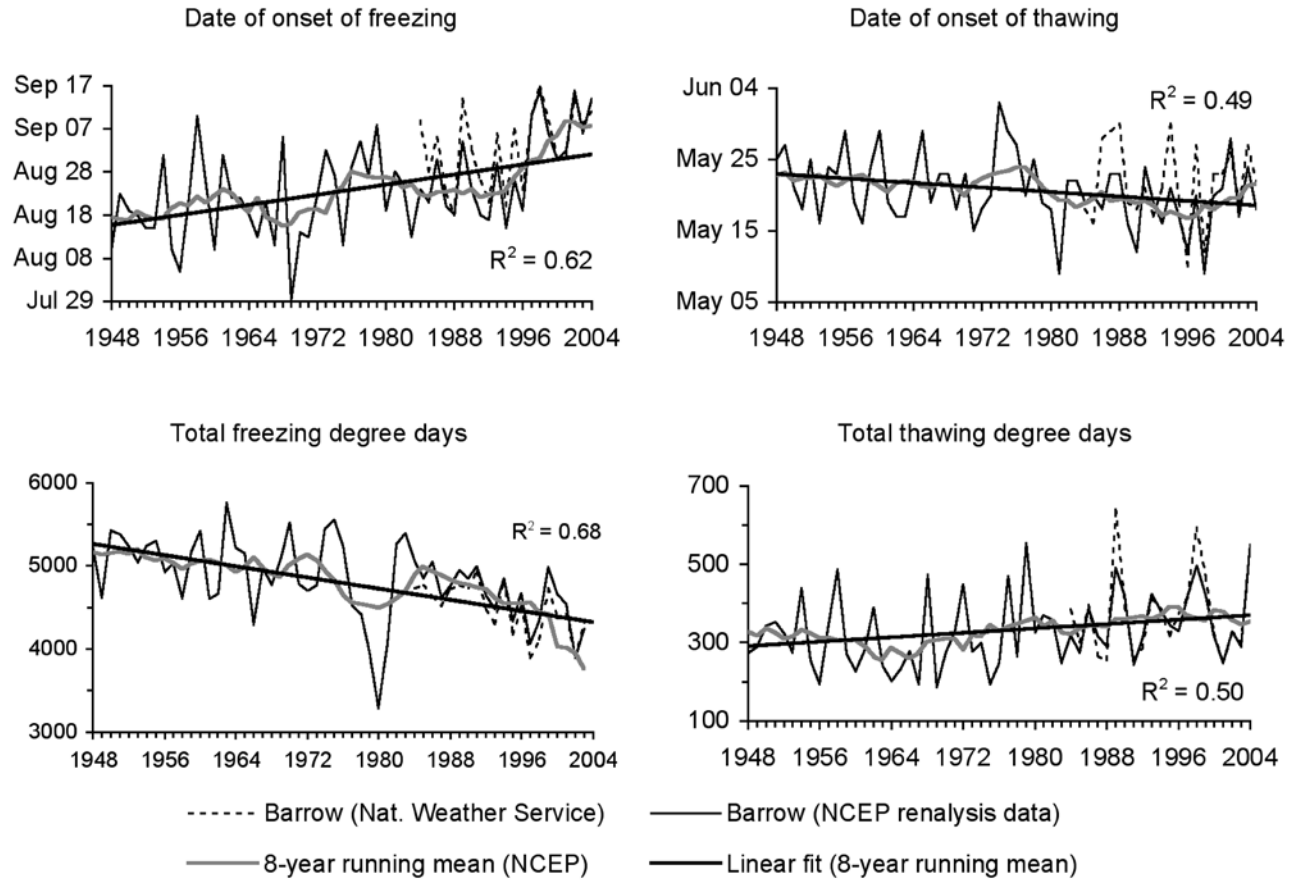

Figure 12. Dates of onset of freezing and thawing and their respective degree day totals for each year. The solid curve denotes values derived from NCEP data, while the dashed line denotes those calculated from Barrow Wiley Post Airport weather station data for the period 1984–2004. Also shown are linear regression lines for the 8-year means.

relationship to the observed differences in the mean annual cycle between this study and that of *Barry* [1979] and *Barry et al.* [1979]. Comparing the 8-year means centered on 1975 (study period of Barry et al.) and 2000 (this study), the onset of freezing occurred 12 days later, while thawing occurred 5 days earlier.

4. Discussion

4.1. Linkages of Landfast Ice Variability With Coastal Morphology and Bathymetry

[44] From our analysis of Radarsat imagery, we characterized the landfast ice of northern Alaska and northwest Canada in terms of its width, the water depth at its seaward edge, and the timing of key events during its annual cycle. In doing so, we observed spatial variability in the character of the landfast ice at different scales. Here, we examine the relationship of SLIE spatial variability with different aspects of coastal morphology and nearshore bathymetry. First, we consider the study area as a whole with regard to typical sea ice drift patterns. In this context Point Barrow is the most important feature of the coast, acting as an obstacle to westward drift of Beaufort Sea pack ice, and placing the Alaskan Chukchi coast in the lee of such drift. Other smaller coastal promontories such as Herschel and Barter Islands have similar effects on sections of the Beaufort Sea Coast.

[45] A leeward coastal aspect promotes the opening of coastal polynyas and shore leads. Such broad areas of open water at the SLIE may help destabilize the landfast ice through two processes. First, during spring, with increasing expanses of open water, incoming shortwave radiation provides approximately 270 Wm^{-2} at Barrow, delivering 250 MJ per linear km of a 1 km wide lead over a 12-hour period (data obtained from the North Slope Atmospheric Radiation Measurement Program). This is sufficient to melt approximately 1 m of ice from a 50 m wide ridge at the SLIE. Although mechanisms for transferring heat from the upper ocean to landfast ice are not well quantified, the solar heating of open water at the SLIE could promote more rapid breakup of landfast ice and result in the accumulation of fewer TDDs prior to break up.

[46] Open water also increases the exposure of the landfast ice to wind waves and swell. Swell can penetrate into an ice cover causing it to break up [*Fox and Squire*, 1990; 1991; *Squire*, 1993; *Langhorne et al.*, 1998]. Although the waves formed in polynyas are typically of much shorter period than are required for this [*Biggs and Willmott*, 2004], field observations by the authors on the landfast ice near Barrow show that sections of landfast ice can break off following the passage of a long period wave across a large expanse of mostly open water.

[47] At smaller scales, embayments and lagoons provide shelter from wind, waves, and drifting ice and therefore promote the more rapid formation of continuous landfast ice (Figure 9). However, there are also river mouths located in many of these embayments, particularly in Zone 2. In the Siberian Arctic, the discharge of rivers is thought to partly control the location of the SLIE [*Dmitrenko et al.*, 1999], but the most noticeable effect of rivers along the Alaska coast appears to be flooding of the landfast ice and promotion of melt in spring. This may explain why fewer TDDs accrue prior to breakup in embayments than headlands in Zone 2 (Figure 9).

[48] Stabilization of the landfast ice relates strongly to the water depth at the SLIE. Consequently, the steepness of the nearshore bathymetry can modulate the impact of coastal morphology on landfast ice behavior. Furthermore, isolated shoals can create leeward regions in a fashion similar to coastal promontories. There are also differences in the weather experienced by different sections of coast in the study area. It is difficult to separate the effects of variability in weather patterns from variability in bathymetry and coastline, but *Eicken et al.* [2006] and *Mahoney* [2006] describe the elements of coastal morphology and bathymetry that may explain differences in landfast behavior that distinguish the four zones identified in this study.

[49] In each zone the landfast ice appears to stabilize at a slightly different depth, but overall, the SLIE typically occupies a narrow range of water depths near the 20 m isobath. The manner in which the SLIE advances into deeper water, with discrete sections advancing first, followed by the surrounding sections (Figure 7), indicates that the SLIE is pinned discontinuously by grounded ridges. From upward looking sonar measurements in waters beyond the landfast ice, *Melling et al.* [1995] calculated that only 0.1% of the ice area exhibits drafts $\geq$20 m and that the pack ice drifts approximately 300 km over the course of the winter. Assuming deep-keeled ridges are on the order of 100 m wide, we could therefore expect grounded ridges approximately every 30 km along the 20 m isobath. Although this corresponds approximately to the spacing of some nodes identified by *Mahoney et al.* [2005], field observations at Barrow [*Mahoney*, 2006] suggest grounded ridges are more closely spaced. Therefore, it seems likely that in situ deformation of landfast ice is important in creating grounded ridges for stabilization.

[50] *Barnes et al.* [1987] observed a pronounced break in bottom slope on the seaward side of shoals near the 20 m isobath, seen as the result of repeated gouging over many years by first-year ridge keels. Barnes et al. propose a feedback mechanism in which the bulldozing action of ice keels helps maintain the shoals, which act as foci for further ice gouging. Their study area was located offshore from Prudhoe Bay very close to a node identified from the combined SLIE data [*Mahoney et al.*, 2005] supporting the notion that such nodes represent grounding locations.

[51] This leaves the question of why grounding and gouging occur so frequently in waters around 20 m deep. *Melling et al.* [1995] show keel abundance decreases rapidly with increasing draft, but ice gouges in the sea bed testify to the existence of keels as deep as 64 m [*Reimnitz et al.*, 1978; *Reimnitz and Barnes*, 1985; *Gilbert and Pederson*, 1987]. This being the case, it is also possible that ridges grounded in greater than 20 m are less capable of stabilizing the SLIE. W. D. Hibler III (personal communication, 2005) suggests that drag exerted by the sea bed on the boundary layer beneath the sea ice may reduce ocean drag on ridge keels in shallow water. However, *Reimnitz et al.* [1978] note an absence of hydraulic bedforms, which would be present if the boundary layer interacted with the sea bed in such a manner.

[52] The feedback mechanism proposed by *Barnes et al.* [1987] suggests that the similarity in location between the SLIE and the 20 m isobath may be a function of the overall configuration of the coast and bathymetry. This notion is supported by the lack of change in the location of the SLIE in recent years, despite changes in Arctic sea ice thickness and extent [*Tucker et al.*, 2001; *Serreze et al.*, 2003; *Stroeve et al.*, 2005]. The fact that other bathymetry relationships occur elsewhere in the Arctic is also consistent with this concept.

4.2. Linkages With Atmospheric Circulation and Air Temperature

[53] There are three different timescales relevant for observations of landfast ice behavior in this study: intra-annual, interannual, and decadal. We observed both intra-annual episodic events and interannual variability between 1996 and 2004. We then compared these observations to earlier, detailed studies from the 1970s to address potential change on decadal timescales. As brief episodic events are the subject of other ongoing research [*Mahoney et al.*, 2007], in this study we will address just the latter two timescales.

[54] *Mahoney et al.* [2005] compared the recent SLIE locations with observations from the 1970s [*Barry et al.*, 1979; *Stringer et al.*, 1980] and found little difference in the late spring/early summer locations of the SLIE. Exceptions occur near Point Barrow and Barter Island where the landfast ice is narrowest and the SLIEs observed in the 1970s lie further offshore. The SLIEs derived by Barry et al. and Stringer et al. were mostly observed in early June, whereas they most strongly resemble the SLIE locations derived for the month of May in this study, which suggests a change in seasonality in recent years. This agrees with the differences in timing and duration of the annual landfast ice cycle discussed in section 3.4. We also note long-term changes in the onsets of freezing and thawing temperatures (section 3.7) and significant differences in the dates of these onsets between the two study periods. To analyze the processes driving the timing of the landfast ice cycle, we will first examine interannual variability between 1996 and 2004.

[55] If stable extensions are excluded, as others have done [*Barry et al.*, 1979; *Stringer et al.*, 1980], landfast ice extent does not appear to vary significantly on an interannual basis. This differs from observations in other Arctic marginal seas. In the Russian Arctic, landfast ice extent has been correlated with the discharge of Ob', Yenisei, Lena, and Kolyma rivers [*Dmitrenko et al.*, 1999]. Also, although they observe no significant long-term trends, *Polyakov et al.* [2003] note that variability in landfast ice extent in the Laptev, East Siberian, and Chukchi Seas correlates with both dynamic and thermodynamic forcing. In the Kara Sea, they suggest that thermodynamic forcing is more important, which differs from the findings of *Divine et al.* [2005], who

Table 5. Correlation and Lags Between Key Landfast Ice Events (Section 2.3) and Measures of Interannual Variability in the Temperature and Atmospheric Circulation

		Correlation	Lag, days			
		R^2	Mean	σ	Min	Max
Onset of freeze	First landfast ice[a]	0.08	60	10.4	47	3
	Stabilization	0.02	147	16.3	128	173
Fall CP Transition	First landfast ice[a]	0.16	60	10.3	45	73
	Stabilization	0.23	143	13.3	130	170
Fall 80% nearshore SIC	First landfast ice[a]	0.72[b]	29	13.1	15	59
	Stabilization	0.07	112	18.4	91	144
Onset of thaw	Breakup	0.68[b]	18	4.6	11	24
	Ice-free coasts	0.72[b]	29	3.7	24	34
Spring CP transition	Breakup	0.34	11	9.8	−4	24
	Ice-free coasts	0.38	23	10.1	9	35
Spring 80% nearshore SIC	Breakup	0.45	−36	15.0	−54	−9
	Ice-free coasts	0.08	−25	15.5	−42	2

[a]Here 1996–1998 omitted from analysis (see section 2.3).
[b]Significant at 95% cutoff.

note that there are modes of Kara Sea landfast ice extent, which are controlled by atmospheric circulation. However, Alaska landfast ice extent appears more narrowly confined by bathymetry and less dependent on climatic forcing, probably due to steeper bathymetric gradients than in the Russian Arctic.

[56] Landfast ice does not form exclusively in situ but relies upon the advection of pack ice to stabilize and increase in area. To examine interannual variability of pack ice interaction, we acquired Defense Meteorological Satellite Program (DMSP) Special Scanner Microwave/Imager (SSM/I) Daily Polar Gridded Sea Ice Concentrations [*Cavalieri et al.*, 1990] for the eight annual cycles of our study period. From these data, we derived estimates of the timing of the appearance and disappearance of pack ice from the nearshore zone. These dates were defined according to when the mean daily sea ice concentration (SIC) in grid cells within 200 km (8 grid cells) of the coast rose above and dropped below a given threshold. We excluded data within 50 km (2 grid cells) of the land to reduce the effects of land contamination. A threshold of 80% SIC was found to yield the strongest correlations with landfast ice behavior.

[57] The start of the landfast ice cycle does not correlate strongly with either the onset of freezing temperatures or the fall transition from summer to winter SLP patterns (Table 5). Also, the number of FDDs acquired prior to the presence of landfast ice (Figure 9) varies greatly between years. However there is a correlation ($R^2 = 0.72$) between the mean date of the first appearance of landfast ice and the date at which the mean SIC in the nearshore rose above 80%. Although this analysis only includes data from five annual cycles due to lack of Radarsat data in early winter of 1996–1998 (section 2.3), the presence of significant concentrations of pack ice in the near-shore zone appears to have strongest direct effect upon landfast ice formation.

[58] The timings of breakup and ice-free coasts in spring are more clearly correlated with temperature and atmospheric circulation. The mean date of onset of thawing temperatures is the strongest corollary for events at the end of the landfast ice season (Table 5). In addition, the mean annual dates of break-up correlate well with those of ice-free coastlines ($R^2 = 0.91$). On average, over the 8 years of the study period, the onset of thawing temperatures occurred 18 days prior to break up and 29 days prior to ice-free coasts. However, despite relatively small standard deviations in lag intervals, the predictive usefulness of this date is limited since lag periods are also small and only slightly larger than the window of time used to calculate onset of thaw (section 2.5).

[59] The correlations of breakup and ice-free coasts with the springtime transition from winter to summer CPs are considerably weaker (Table 5), which suggests that the end of the annual landfast ice cycle is controlled more by thermodynamics than atmospheric dynamics. In addition, there is less variability in the TDDs required for breakup and ice-free conditions as compared with FDDs required for the formation of landfast ice (Figure 9). The TDD totals for each event are within the same range as those determined by *Barry et al.* [1978] and *Barry et al.* [1979]. However, no correlation could be found that might suggest an underlying cause for interannual variability in the number of TDDs acquired prior to breakup and ice-free conditions.

[60] In the above analysis, we have identified the main variables that explain the interannual variability in the timing of landfast ice events between 1996 and 2004. This has been achieved through correlation of mean annual measures of atmospheric circulation, pack ice concentration and air temperature with mean dates of landfast ice events. However, in doing so, we have neglected climatic differences across the study area. This may explain the weak correlations found at the beginning of the landfast ice cycle. Additional analyses were performed on individual zones, but this did not significantly improve the correlations. The CP analysis cannot be broken down in this way and so does not take into account differences between zones. For instance, the Chukchi Sea coast experiences the influence of Bering Sea storms more directly than the Beaufort coast throughout the landfast ice season [*Atkinson*, 2005]. Such storms are not well captured by the CP analysis. The response of landfast ice to climate forcing in the Chukchi Sea probably explains one half of the ''u''- and ''n''-shaped date curves in Figure 8 and the greater level of interannual variability of key event dates (Table 3).

[61] In examining differences between the dates of key events identified in this study (section 3.4) and those of the 1973–1977 [*Barry et al.*, 1979], we take into account some of these regional differences. Thus landfast ice formation occurs up to 1 month later in Zone 1, while Zone 2 shows little change from the earlier period. The mean standard deviations of dates in Zone 1 are significantly larger than in Zone 2, such that the difference between study periods lies within the range of uncertainty. Furthermore, it is unclear what may be responsible for such a change due to weak correlations with the date of landfast ice formation. Thus although Figure 12 shows a trend toward a later onset of freezing temperatures, it is not clear whether this is related to any change in the landfast ice season.

[62] In spring, it is in the Beaufort Sea that the greatest differences occur between study periods, though both Zone 1 and 2 show earlier breakup and ice-free conditions in recent years, particularly if the first dates of breakup within each zone are used (section 3.4). In agreement with *Barry et al.* [1978] and *Barry* [1979], the results of this study show that the timing of landfast ice breakup

correlates most closely with air temperature and thawing degree days. However, this is not to say that turbulent heat flux from the atmosphere is the main driving mechanism behind melting and breakup since the other processes in the surface energy balance also control the accumulation thawing degree days. Breaking up of sea ice can provide positive feedback on air temperature since more open water in the ice cover will increase the shortwave flux, raising surface air temperature. We therefore suggest that the long-term trend towards an earlier onset of thawing (Figure 12) is evidence that the shortening of the landfast ice year in spring is also part of a longer term trend.

5. Conclusions

[63] Using Radarsat SAR imagery, we identified the extent of landfast sea ice along the coasts of northern Alaska and northwestern Canada and observed its annual cycles between 1996 and 2004. By defining four key events within the annual cycle, we have produced a detailed climatology of landfast ice and its variability along the northern Alaska coastline. We also compared the timing of these key events with similar observations for the period 1973–1977 [*Barry et al.*, 1979]. In those years for which we were able to acquire SAR imagery early enough in the season (1999–2003), we found that landfast ice formed approximately 1 month later along the Alaska Chukchi Coast than it did in the 1970s, though this was within the range of uncertainty. Landfast ice in the western Beaufort Sea exhibited no significant change in formation date. In spring, the mean date of breakup was 6 days earlier than during the period 1973–1977 along the Chukchi Coast and 19 days earlier along the Beaufort Coast. We may have underestimated the difference in breakup dates by up to 3 weeks by calculating the mean date along a section of coast instead of the date of the first sign of breakup. Overall, our results indicate a shortening of the landfast ice season that will have implications for subsistence and commercial activities in this region. In addition, this is likely to lead to increased coastal erosion.

[64] Between 1999 and 2003 (SAR imagery was not available to capture formation in 1996–1998), onset of landfast ice formation correlated most strongly with the timing of pack ice incursion into coastal waters. Therefore the later formation of landfast ice in recent years may relate to the northward migration of the perennial sea ice edge [*Serreze et al.*, 2003; *Stroeve et al.*, 2005]. Breakup and the onset of ice-free coasts were observed in all 8 years of the study (1997–2004) and correlated strongly with the onset of thawing mean daily air temperatures. In addition, using NCEP data from the period 1948–2004, we observed a multidecadal trend toward a later onset of thawing, from which we conclude that the earlier decay of landfast ice is likely to be part of a long-term trend.

[65] In terms of overall extent of landfast ice, we did not note any significant difference between recent years and the 1970s, although we observed broad stable extensions of landfast sea ice of a scale and persistence that had not been reported before. These extensions persisted for between 30 and 50 days and extended hundreds of kilometers from the coast. No corollary to their occurrence was found in the characteristic SLP patterns. While these extensions are not usually considered as part of the landfast ice from an operational standpoint, they represent a persistent physical barrier isolating the waters beneath from the atmosphere above, with potentially significant oceanographic and ecological implications.

[66] Despite regional differences in other aspects of landfast ice behavior, the landfast ice terminates at approximately 20 m of water throughout the study area. This observation has been made by many authors [*Reimnitz and Barnes*, 1974; *Shapiro*, 1976; *Kovacs*, 1976; *Stringer et al.*, 1980; *Barnes et al.*, 1987] but in this study we have quantified the relationship and its spatial and temporal variability. Furthermore, we show that reaching an isobath near 20 m is a critical event in the annual cycle allowing the advance of neighboring landfast ice to this depth and in turn the subsequent advance of the SLIE into deeper water.

[67] The relationship between the location of the SLIE and isobaths near 20 m is strong evidence for the importance of grounded ridges in stabilizing the SLIE. However, questions remain as to why grounding is so much less frequent beyond the 20 m isobath when there is evidence that deeper keels exist. It seems likely that either there is an abrupt decrease in the abundance of keels deeper than 20 m, as suggested by *Melling et al.* [1995], or that the ridge keels experience greater ocean drag in deeper water (W. D. Hibler III, personal communication, 2005). Understanding the mechanisms by which grounded ridges hold sea ice fast to the coast is important in predicting the response of landfast ice to the Arctic sea ice changes observed in recent years [e.g., *Tucker et al.*, 2001; *Perovich et al.*, 2003; *Serreze et al.*, 2003; *Stroeve et al.*, 2005].

[68] **Acknowledgments.** This work was funded by the Mineral Management Service under MMS contract 0103CT71707. We would also like to acknowledge the Alaska Satellite Facility, particularly Rudi Gens, for meeting our needs regarding Radarsat data. We are also grateful to R. Barry and R. Moritz for helping provide details on work from the 1970s. Constructive comments by three anonymous reviewers and Associate Editor B. Tremblay are gratefully acknowledged.

References

Atkinson, D. E. (2005), Observed storminess patterns and trends in the circum-Arctic coastal regime, *Geo Mar. Lett.*, *25*, 98–109.

Barnes, P. W., J. L. Asbury, D. M. Rearic, and C. R. Ross (1987), Ice erosion of a sea-floor knickpoint at the inner edge of the Stamukhi Zone Beaufort Sea, Alaska, *Mar. Geol.*, *76*, 207–222.

Barnett, D. (1991) Sea ice distribution in the Soviet Arctic, in *The Soviet Maritime Arctic*, edited by L. W. Brigham, pp. 47–62, Belhaven Press, London.

Barry, R. (1979), Study of climatic effects on fast ice extent and its seasonal decay along the Beaufort-Chukchi coasts, in *Environmental Assessment of the Alaskan Continental Shelf*, *Phys. Sci. Stud.*, vol. 2, final report, pp. 272–375, Environ. Res. Lab., Boulder, Colo.

Barry, R. G., and A. M. Carleton (2001), *Synoptic and Dynamic Climatology*, 552 pp., Routledge, Boca Raton, Fla.

Barry, R. G., J. D. Jacobs, R. G. Crane, R. A. Keen, R. E. Mortiz, E. F. LeDrew, and R. L. Weaver (1978), Energy budget studies in relation to fast-ice breakup processes in Davis Strait: A climatological overview, report, Inst. of Arct. and Alpine Res. Univ. of Colo., Boulder.

Barry, R. G., R. E. Moritz, and J. C. Rogers (1979), The fast ice regimes of the Beaufort and Chukchi sea coasts, Alaska, *Cold Reg. Sci. Technol.*, *1*, 129–152.

Biggs, N. R. T., and A. J. Willmott (2004), Unsteady polynya flux model solutions incorporating a parameterization for the collection thickness of consolidated new ice, *Ocean Modell. 7*, Hooke Inst. Oxford Univ., Oxford, U. K.

Blazey, B., A. Mahoney, and H. Eicken (2005), Landfast ice breakouts on the northern Alaskan coast, *Eos Trans. AGU*, *86*(52), Fall Meet. Suppl., Abstract C41B-0197.

Canadian Hydrographic Service (1968), Pilot of Arctic Canada, report, Surv. and Mapp. Branch Dept. of Mines and Tech. Surv., Ottawa.

Cavalieri, D. J., P. Gloersen and H. J. Zwally (1990), DMSP SSM/I daily polar gridded sea ice concentrations, http://nsidc.org/data/nsidc-0002.html, National Snow and Ice Data Cent., Boulder, Colo.

Divine, D., R. Korsnes, and A. Makshtas (2004), Temporal and spatial variations of shore-fast ice in the Kara Sea, *Cont. Shelf Res.*, *24*, 1717–1736.

Divine, D. V., R. Korsnes, A. P. Makshtas, F. Godtliebsen, and H. Svendsen (2005), Atmospheric-driven state transfer of shore-fast ice in the north-eastern Kara Sea, *J. Geophys. Res.*, *110*, C09013, doi:10.1029/2004JC002706.

Dmitrenko, I. A., V. A. Gribanov, D. L. Volkov, H. Kassens, and H. Eicken (1999), Impact of river discharge on the fast ice extension in the Russian Arctic shelf area, in *Proceedings of the 15th International Conference on Port and Ocean Engineering under Arctic Conditions (POAC99), Helsinki, 23–27 August, 1999*, vol. 1, pp. 311–321, Helsinki Univ. of Technol., Helsinki, Finland.

Eicken, H., I. Dmitrenko, K. Tyshko, A. Darovskikh, W. Dierking, U. Blahak, J. Groves, and H. Kassens (2005), Zonation of the Laptev Sea landfast ice cover and its importance in a frozen estuary, *Global Planet. Change*, *48*, 55–83.

Eicken, H., L. Shapiro, A. Gaylord, A. Mahoney, and P. Cotter (2006), Mapping and characterization of recurring spring leads and landfast ice in the Beaufort and Chukchi Seas, final report, OCS Study MMS 2005-068, 180 pp., Min. Manage. Serv., U.S. Dept. of the Interior, Anchorage, Alaska.

Fox, C., and V. Squire (1990), Reflection and transmission characteristics at the edge of shore fast sea ice, *J. Geophys. Res.*, *95*, 11,629–11,639.

Fox, C., and V. Squire (1991), Strain in shore fast ice due to incoming ocean waves and swell, *J. Geophys. Res.*, *96*, 4531–4547.

George, J. C., H. P. Huntington, K. Brewster, H. Eicken, D. W. Norton, and R. Glenn (2004), Observations on shorefast ice dynamics in Arctic Alaska and the responses of the Iñupiat hunting community, *Arctic*, *57*, 363–374.

Gilbert, G., and K. Pederson (1987), Ice scour database for the Beaufort Sea, *Rep. 055*, 99 pp., Environ. Stud. Revolving Funds, Ottawa.

Jacobs, J. D., R. G. Barry, and R. L. Weaver (1975), Fast ice characteristics, with special reference to the eastern Canadian Arctic, *Polar Rec.*, *110*, 521–536.

Kirchhofer, W. (1974), Classification of European 500 Mb patterns, *Schwiez. Meteorol. Anstalt Inst. Suisse Meteorol. Zurich*, *43*, 1–16.

Kovacs, A. (1976), Grounded ice in the fast ice zone along the Beaufort Sea coast of Alaska, *Rep. 76-32*, Cold Regions Res. and Environ. Lab., Hanover, N. H.

Kovacs, A., and M. Mellor (1974), Sea ice geomorphology and ice as a geologic agent in the northern Beaufort Sea, in *The Coast and Shelf of the Beaufort Sea*, edited by J. C Reed and J. E. Sater, pp. 113–162, Arct. Inst. of North Am., Arlington, Va.

Langhorne, P., V. Squire, C. Fox, and T. G. Haskell (1998), Break-up of sea ice by ocean waves, *Ann. Glaciol.*, *27*, 439–442.

Mahoney, A. (2006), Alaska landfast sea ice dynamics, Ph.D. thesis, 152 pp., Univ. of Alaska, Fairbanks.

Mahoney, A., H. Eicken, A. G. Gaylord, L. Shapiro, and P. Cotter (2004), Landfast sea ice extent and variability in the Alaskan Arctic derived from SAR imagery, in *International Geoscience and Remote Sensing Symposium, Anchorage, Alaska*, vol. 3, pp. 2146–2149, IEEE, Anchorage, Alaska.

Mahoney, A., H. Eicken, L. Shapiro, and A. Graves (2005), Defining and locating the seaward landfast ice edge in northern Alaska, paper presented at the 18th International Conference on Port and Ocean Engineering under Arctic Conditions, Clarkson Univ., Potsdam, New York, 26–30 June.

Mahoney, A., H. Eicken, and L. S. Shapiro (2007), How fast is landfast sea ice?: A study of the attachment and detachment of sea ice near Barrow, Alaska, *Cold Regions Sci. Technol.*, in press.

Melling, H., P. H. Johnston, and D. A. Riedel (1995), Measurements of the underside topography of sea ice by moored subsea sonar, *J. Atmos. Oceanic Technol.*, *12*, 589–602.

Moritz, R. E. (1979) Synoptic climatology of the Beaufort Sea coast of Alaska, *Occasional Pap. 30*, 176 pp., Inst. of Arct. and Alpine Res. Univ. of Colo., Boulder.

Nelson, R. K. (1969) *Hunters of the Northern Ice*, Univ. of Chicago Press, Chicago, Ill.

Perovich, D. K., T. C. Grenfell, J. A. Richter-Menge, W. B. Tucker III, B. Light, and H. Eicken (2003), Thin and thinner: Sea ice mass balance measurements during SHEBA, *J. Geophys. Res.*, *108*(C3), 8050, doi:10.1029/2001JC001079.

Persson, P. O. G., C. W. Fairall, E. L. Andreas, P. S. Guest, and D. K. Perovich (2002), Measurements near the Atmospheric Surface Flux Group tower at SHEBA: Near-surface conditions and surface energy budget, *J. Geophys. Res.*, *107*(C10), 8045, doi:10.1029/2000JC000705.

Polyakov, I., G. V. Alekseev, R. V. Bekryaev, U. S. Bhatt, R. L. Colony, M. A. Johnson, V. P. Karklin, D. Walsh, and A. V. Yulin (2003), Long-term ice variability in Arctic marginal seas, *J. Clim.*, *16*, 2078–2085.

Reimnitz, E. (2000), Interactions of river discharge with sea ice in proximity of Arctic deltas: A review, *Polarforschung*, *70*, 123–134.

Reimnitz, E., and P. Barnes (1974), Sea ice as a geologic agent on the Beaufort Sea shelf of Alaska, in *The Coast and Shelf of the Beaufort Sea (Proceedings of a Symposium on Beaufort Sea Coast and Shelf Research)*, edited by J. C. Reed and A. G. Slater, pp. 301–353, Arct. Inst. of North Am., Arlington, Va.

Reimnitz, E., and P. Barnes (1985), Determining the maximum keel depth in the Arctic Ocean, paper WV117-125 presented at the Arctic Energy Technologies Conference, U.S. Dept. of Energy, Morgantown, W. V.

Reimnitz, E., L. J. Toimil, and P. W. Barnes (1978), Arctic continental shelf morphology related to sea ice zonation Beaufort Sea, Alaska, *Mar. Geol.*, *28*, 179–210.

Reimnitz, E., H. Eicken, and T. Martin (1995), Multi-year fast ice along the Taymyr peninsula, Siberia, *Arctic*, *48*, 359–367.

Serreze, M. C., and A. Etringer (2003), Precipitation characteristics of the Eurasian Arctic drainage system, *Int. J. Climatol.*, *23*, 1267–1291.

Serreze, M. C., J. A. Maslanik, T. A. Scambos, F. Fetterer, J. Stroeve, K. Knowles, C. Fowler, S. Drobot, R. G. Barry, and T. M. Haran (2003), A record minimum Arctic sea ice extent and area in 2002, *Geophys. Res. Lett.*, *30*(3), 1110, doi:10.1029/2002GL016406.

Shapiro, L. H. (1976), A preliminary study of ridging in landfast ice at Barrow, Alaska, using radar data, in *3rd International Conference on Port and Ocean Engineering under Arctic Conditions*, vol. 1, pp. 417–425, Univ. of Alaska, Fairbanks, Alaska.

Squire, V. A. (1993), The breakup of shore fast sea ice, *Cold Reg. Sci. Technol.*, *21*, 211–218.

Stringer, W. J. (1974), Morphology of the Beaufort Sea shorefast ice, in *The Coast and Shelf of the Beaufort Sea*, edited by J. C. Reed and J. E. Sater, pp. 165–172, Arct. Inst. of North Am., Arlington, Va.

Stringer, W. J., S. A. Barrett, and L. K. Schreurs (1980) *Nearshore Ice Conditions and Hazards in the Beaufort, Chukchi and Bering Seas*, 96 pp., Geophys. Inst. Univ. of Alaska, Fairbanks.

Stroeve, J. C., M. C. Serreze, F. Fetterer, T. Arbetter, W. Meier, J. Maslanik, and K. Knowles (2005), Tracking the Arctic's shrinking ice cover: Another extreme September minimum in 2004, *Geophys. Res. Lett.*, *32*, L04501, doi:10.1029/2004GL021810.

Thorndike, A. S., and R. Colony (1982), Sea ice motion in response to geostrophic winds, *J. Geophys. Res.*, *87*, 5845–5852.

Tucker, W. B. I., J. W. Weatherly, D. T. Eppler, D. Farmer, and D. L. Bentley (2001), Evidence for the rapid thinning of sea ice in the western Arctic Ocean at the end of the 1980s, *Geophys. Res. Lett.*, *28*, 2851–2854.

Weeks, W. F., A. Kovacs, S. J. Mock, W. B. Tucker, W. D. Hibler III, and A. J. Gow (1977), Studies of the movement of coastal sea ice near Prudhoe Bay, Alaska, U.S.A., *J. Glaciol.*, *19*, 533–546.

Zubov, N. N. (1945), *Arctic Sea Ice* (in Russian), 366 pp., Izd. Glavsevmorputi, Moscow. (English translation, 491 pp., U.S. Navy Oceanogr. Off., Springfield, Va., 1963.)

H. Eicken and L. Shapiro, Geophysical Institute, University of Alaska Fairbanks, Fairbanks, AK 99775, USA.

A. G. Gaylord, Nuna Technologies, P. O. Box 1483, Homer, AK 99603, USA.

A. Mahoney, National Snow and Ice Data Center, 1540 30th Street RL-2, Boulder, CO 80303, USA. (andrew.mahoney@nsidc.org)